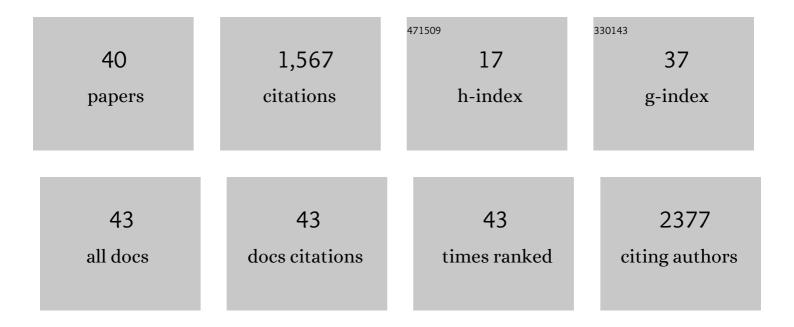
Karen C Bustillo

List of Publications by Year in descending order

Source: https://exaly.com/author-pdf/3399491/publications.pdf Version: 2024-02-01



#	Article	IF	CITATIONS
1	Cryogenic 4D-STEM analysis of an amorphous-crystalline polymer blend: Combined nanocrystalline and amorphous phase mapping. IScience, 2022, 25, 103882.	4.1	7
2	Response to Comment on "Reversible disorder-order transitions in atomic crystal nucleation― Science, 2022, 375, eabj3683.	12.6	0
3	Defect-mediated ripening of core-shell nanostructures. Nature Communications, 2022, 13, 2211.	12.8	17
4	Dynamics of Polymer Nanocapsule Buckling and Collapse Revealed by <i>In Situ</i> Liquid-Phase TEM. Langmuir, 2022, 38, 7168-7178.	3.5	5
5	Hard Ferromagnetism Down to the Thinnest Limit of Iron-Intercalated Tantalum Disulfide. Journal of the American Chemical Society, 2022, 144, 12167-12176.	13.7	19
6	Identification of a quasi-liquid phase at solidâ \in "liquid interface. Nature Communications, 2022, 13, .	12.8	15
7	Reversible disorder-order transitions in atomic crystal nucleation. Science, 2021, 371, 498-503.	12.6	117
8	Strain fields in twisted bilayer graphene. Nature Materials, 2021, 20, 956-963.	27.5	126
9	py4DSTEM: A Software Package for Four-Dimensional Scanning Transmission Electron Microscopy Data Analysis. Microscopy and Microanalysis, 2021, 27, 712-743.	0.4	121
10	4D-STEM of Beam-Sensitive Materials. Accounts of Chemical Research, 2021, 54, 2543-2551.	15.6	48
11	Observation of Surface Ligands-Controlled Etching of Palladium Nanocrystals. Nano Letters, 2021, 21, 6640-6647.	9.1	10
12	Multibeam Electron Diffraction. Microscopy and Microanalysis, 2021, 27, 129-139.	0.4	9
13	Tetragonal CoMn ₂ O ₄ nanocrystals on electrospun carbon fibers as high-performance battery-type supercapacitor electrode materials. Dalton Transactions, 2021, 50, 15669-15678.	3.3	7
14	A strain-driven thermotropic phase boundary in BaTiO3 at room temperature by cycling compression. AIP Advances, 2021, 11, 115122.	1.3	0
15	A unique pathway of PtNi nanoparticle formation observed with liquid cell transmission electron microscopy. Nanoscale, 2020, 12, 1414-1418.	5.6	7
16	Patterned probes for high precision 4D-STEM bragg measurements. Ultramicroscopy, 2020, 209, 112890.	1.9	61
17	4DSTEM of Beam-sensitive Materials: Optimizing SNR and Improving Spatial Resolution. Microscopy and Microanalysis, 2020, 26, 1734-1735.	0.4	2
18	Hybrid nanocapsules for <i>in situ</i> TEM imaging of gas evolution reactions in confined liquids. Nanoscale, 2020, 12, 18606-18615.	5.6	4

KAREN C BUSTILLO

#	Article	IF	CITATIONS
19	Scanning Nanobeam Diffraction and Energy Dispersive Spectroscopy Characterization of a Model Mn-Promoted Co/Al ₂ O ₃ Nanosphere Catalyst for Fischer–Tropsch Synthesis. ACS Catalysis, 2020, 10, 12071-12079.	11.2	7
20	Determining Atomic Structures from Digitally Defined Regions of Nanocrystals. Microscopy and Microanalysis, 2020, 26, 748-749.	0.4	0
21	Atomic structures determined from digitally defined nanocrystalline regions. IUCrJ, 2020, 7, 490-499.	2.2	8
22	Formation of two-dimensional transition metal oxide nanosheets with nanoparticles as intermediates. Nature Materials, 2019, 18, 970-976.	27.5	169
23	Hierarchically-structured large superelastic deformation in ferroelastic-ferroelectrics. Acta Materialia, 2019, 181, 501-509.	7.9	20
24	Palladium oxidation leads to methane combustion activity: Effects of particle size and alloying with platinum. Journal of Chemical Physics, 2019, 151, 154703.	3.0	30
25	Detailed Investigation of Silicon Nitride Phase Plates Prepared by Focused Ion Beam Milling. Microscopy and Microanalysis, 2019, 25, 900-901.	0.4	1
26	Nanoscale mosaicity revealed in peptide microcrystals by scanning electron nanodiffraction. Communications Biology, 2019, 2, 26.	4.4	47
27	Diffraction imaging of nanocrystalline structures in organic semiconductor molecular thin films. Nature Materials, 2019, 18, 860-865.	27.5	99
28	Direct imaging of short-range order and its impact on deformation in Ti-6Al. Science Advances, 2019, 5, eaax2799.	10.3	86
29	Anomalous Shape Evolution of Ag ₂ O ₂ Nanocrystals Modulated by Surface Adsorbates during Electron Beam Etching. Nano Letters, 2019, 19, 591-597.	9.1	2
30	Selective nitrogen doping of graphene oxide by laser irradiation for enhanced hydrogen evolution activity. Chemical Communications, 2018, 54, 13726-13729.	4.1	28
31	Growth mechanism of core–shell PtNi–Ni nanoparticles using in situ transmission electron microscopy. Nanoscale, 2018, 10, 11281-11286.	5.6	15
32	Quantitative characterization of high temperature oxidation using electron tomography and energy-dispersive X-ray spectroscopy. Scientific Reports, 2018, 8, 10239.	3.3	6
33	A spongy nickel-organic CO ₂ reduction photocatalyst for nearly 100% selective CO production. Science Advances, 2017, 3, e1700921.	10.3	175
34	Growth and assembly of cobalt oxide nanoparticle rings at liquid nanodroplets with solid junction. Nanoscale, 2017, 9, 13915-13921.	5.6	10
35	Nanobeam Scanning Diffraction for Orientation Mapping of Polymers. Microscopy and Microanalysis, 2017, 23, 1782-1783.	0.4	7
36	Development of Diffraction Scanning Techniques for Beam Sensitive Polymers Microscopy and Microanalysis, 2016, 22, 492-493.	0.4	2

KAREN C BUSTILLO

#	Article	IF	CITATIONS
37	Orientation mapping of semicrystalline polymers using scanning electron nanobeam diffraction. Micron, 2016, 88, 30-36.	2.2	54
38	In Situ Study of Lithiation and Delithiation of MoS ₂ Nanosheets Using Electrochemical Liquid Cell Transmission Electron Microscopy. Nano Letters, 2015, 15, 5214-5220.	9.1	135
39	In Situ Study of Spinel Ferrite Nanocrystal Growth Using Liquid Cell Transmission Electron Microscopy. Chemistry of Materials, 2015, 27, 8146-8152.	6.7	39
40	In Situ Study of Fe ₃ Pt–Fe ₂ O ₃ Core–Shell Nanoparticle Formation. Journal of the American Chemical Society, 2015, 137, 14850-14853.	13.7	51